Journal of Optics
https://doi.org/10.1007/s12596-025-02990-3

RESEARCH ARTICLE

Heterodyne spectroscopy using comb and tunable laser with low-speed detector

Zhen Zhang[1,2] · Qiuwei Xia[1,2] · Haobin Han[1] · Yixiang Chen[1] · Saifen Yu[1,2] · Haiyun Xia[1,2]

Received: 12 December 2024 / Accepted: 6 November 2025

Abstract
Heterodyne spectroscopy using comb and continuous-wave (CW) gives a highly sensitive and accurate way to measure the absorption spectrum with resolved comb lines. Here, to avoid using a high-speed optical detector and ADC card, low-bandwidth heterodyne spectroscopy is demonstrated by using a tunable CW laser and a probing comb laser, realizing easy data acquisition, real-time storage, and processing. The absolute frequency accuracy of the CW laser is guaranteed by locking the laser to one of the optical frequency comb teeth. And the multi-heterodyne beats within a bandwidth of 350 MHz are acquired at each sampling frequency step. The beat signal between comb teeth is suppressed by introducing a dispersion compensation fiber, avoiding its confusion between the multi-heterodyne signal. Two working modes, the wideband searching mode and the precise analyzing mode are integrated for fast searching the gas absorption spectrum over a wideband range and analyzing the absorption feature within a determined span. In experiment, the $H^{13}CN$ absorption spectrum is analyzed with spectrum resolution equal to the comb tooth spacing of 100 MHz. The maximum relative deviation of the spectral transmittance is approximately 3%, with a time resolution of 400 μs per sampling step and an acquisition time of about 2 ms for a single absorption line.

Keywords Frequency comb · High-speed detection

Introduction

Optical frequency (OF) combs have revolutionized frequency metrology and opened up new opportunities for clock [1], spectroscopy [2], and radio-frequency arbitrary waveform generation [3] in the past decades. In particular, spectroscopy with frequency comb offers marked improvements in spectral resolution, range, and sensitivity. For example, the multi-heterodyne spectroscopy [4], builds a direct link between OF combs and radio frequency (RF) comb without moving parts. Dual-comb spectroscopy [4, 5] generates the multi-heterodyne beat notes by utilizing two frequency combs with slightly different repetition rates. It not only down-converts the spectrum from OF domain to RF domain but also compresses the spectrum span from tens of THz to hundreds of MHz with compression factors of 30,000–1,000,000 [5]. Additionally, researchers have devoted to simplifying the comb system with cutting-edge techniques, such as single-cavity dual-comb lasers [6–8], electro-optic modulation combs [9, 10], and microresonator frequency combs [11].

Besides dual-comb interferometry, multiple comb-resolved spectra also can be generated by the interference between a comb and a continuous-wave (CW) laser. The CW laser interferes with the wideband comb and down-converts the comb spectrum information to the RF domain [12–16]. This kind of multi-heterodyne spectroscopy has higher sensitivity because the power per mode of the CW laser is much higher than the local comb in dual-comb spectroscopy [15]. The enhancement is at the expense of the spectral bandwidth, because an absorption spectrum with a span of tens of gigahertz should be detected and sampled without compressing [14]. It is not economical to analyze the absorption spectrum over a broad spectrum range. However,

✉ Saifen Yu
sfyu@nuist.edu.cn

Haiyun Xia
hsia@ustc.edu.cn

[1] School of Atmospheric Physics, Nanjing University of Information Science and Technology, Nanjing 210044, China

[2] National center of carbon metrology (Fujian), Nanping 353011, China

Published online: 28 November 2025

the requirement of acquisition bandwidth can be reduced by scanning the frequency of CW laser. In order to reduce the frequency noise, the CW laser should be scanned and locked step by step. Fortunately, the frequency comb can serve as not only a wideband probing laser but also a frequency ruler.

In this paper, multi-heterodyne spectroscopy with low acquisition RF bandwidth is demonstrated by combining a comb-referenced tunable CW laser and a direct-comb probe laser. First, the CW laser is referenced by a comb, limiting its frequency uncertainty (standard deviation) to less than 1.06 MHz during an integration time of 50 s. The changing of its frequency is recorded in the trajectory of the beat frequency between the CW laser and the nearest comb tooth. The programmed locking and scanning process is realized in the span of the comb spectrum. Second, the absorption spectrum encoded in the probe comb laser is down-converted to the RF domain by heterodyne detection with the CW laser. Only the RF signal within low bandwidth (350 MHz) is acquired and sampled. The gas absorption line with a span of tens of GHz is analyzed by scanning the CW frequency. Third, to simplify the RF signal processing, the beat signal between two comb teeth which contains no required information is suppressed by introducing the dispersion compensation fiber (DCF).

In addition, it is more comprehensive in practical applications that the spectrum is first searched roughly over a wide range and then analyzed precisely within a determined span. Taking advantage of the proposed frequency scanning and locking method, two working modes are demonstrated in the experiment. Wideband searching mode: the CW laser is fast free scanned in a span of 400 GHz to search the absorption spectrum under test. Precise analyzing mode: the CW laser is locked in 5 frequency steps to sample the P11 line in the $2\nu_3$ band of $H^{13}CN$.

The remainder of the paper is organized as follows. In "Principle and Instrument" section, the principle and optical layout are introduced. The CW frequency tuning and locking method is introduced in "Frequency tuning and locking" section. The suppression of the beats between comb teeth is discussed in "Suppression of the beats between comb teeth" section. The experiment results of two working modes are presented in "Wideband searching and precise detecting modes" section. Finally, a summary is provided in "Conclusion" section.

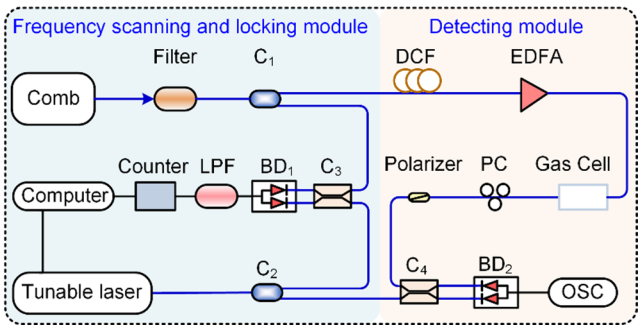

Fig. 1 Optical layout. *C*: coupler. *BD*: balanced detector. *LPF* low-pass filter. *DCF* dispersion compensation fiber. *EDFA* erbium-doped fiber amplifier. *PC* polarization controller. *OSC* oscilloscope

Principle and instrument

Figure 1 outlines the optical layout of the low-bandwidth multi-heterodyne spectroscopy. A home-made optical frequency comb serves as both the frequency calibration ruler and the probing laser. The repetition frequency and the carrier-envelope offset frequency of the comb are $f_r = 100$ MHz and $f_{ceo} = 20$ MHz, respectively. Both f_r and f_{ceo} are phase locked to a microwave rubidium clock. The frequency stability of fceo reaches 1.2×10^{-9} and 2.4×10^{-11} at an integration time of 1 s and 1000 s, respectively. The spectrum of comb and scanning range of CW laser cover the C and L bands, which contain abundant gas absorption features. First, a programmable filter is used to tailor the comb spectrum to the range of interest. Then, both the comb and the CW laser are split into the frequency scanning and locking module and the multi-heterodyne detection module. In the frequency scanning and locking module, the beat signal is received by a balanced detector and filtered by an LPF with a bandwidth of 48 MHz, such that only the beat note generated by the CW laser and the nearest comb tooth is read by a frequency counter. The beat signal is recorded by a computer and used as a feedback signal to control the tunable CW laser.

In the detecting module, the femtosecond pulses first transmit through a DCF with a dispersion value of 8.9 ns/nm and then amplified by an EDFA with a gain of 35 dB. The time-stretch technique of femtosecond pulse has been applied for ultrafast gas detection [8], ranging [17, 18], imaging [19], and soliton observation [20, 21]. Interestingly, the DCF used in this experiment can not only stretch the pulse to obtain higher amplified pulse energy but also has a suppression effect on the beats between comb teeth. The comb transmits through a $H^{13}CN$ gas cell with a length of 48 cm and pressure of 100 Torr. After going through polarization controllers and in-line polarizers, the comb is combined with the CW laser by a 3dB coupler. The multi-heterodyne beats are received by a balanced detector with a bandwidth of 350 MHz. Actually, the multi-heterodyne detection generates a wide-band RF comb. One can get tens of GHz optical spectrum by a high-speed detector and ADC card. While in this method, to reduce the need of acquisition bandwidth, only the low-frequency part of the multi-heterodyne beat notes is detected.

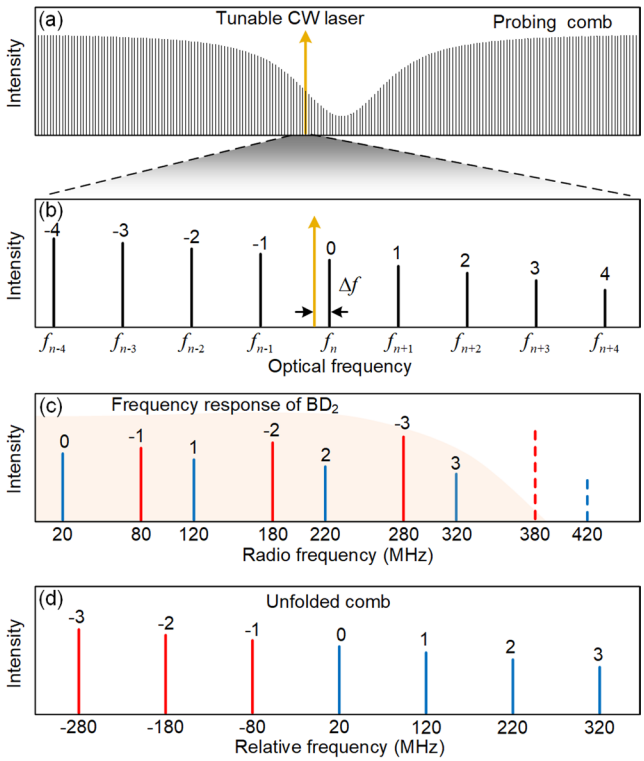

Fig. 2 Principle of multi-heterodyne detection. **a** The spectrum of probing comb encoded with gas absorption feature. **b** The comb-referenced CW laser and the comb teeth around the CW laser. $\Delta f = 20$ MHz is the locking offset frequency. **c** The multi-heterodyne beats generated in **b**. **d** The unfolded comb spectrum relative to the CW frequency

The principle of multi-heterodyne detection at one CW frequency step is illustrated in Fig. 2a, b as a representative. The CW frequency is locked to the comb.

tooth $f_n = nf_r + f_0$ with a locking offset frequency $\Delta f = 20$ MHz. So that the locked CW frequency can be expressed as $f_{CW} = nf_r + f_0 - \Delta f$, where n is the comb tooth number, $f_0$is the carrier-envelope offset frequency. After the CW-comb multi-heterodyne detection, RF comb teeth are generated in the balanced detector. As shown in Fig. 2c, the RF comb with marked numbers represent the spectrum information in the optical frequency comb with the same number in Fig. 2b. The beat notes between f_{CW} and the comb teeth on both sides are folded in the RF domain. To obtain the optical spectrum, the RF comb should be unfolded according to the marked number. The unfolded comb teeth in Fig. 2d represensthe the optical frequency comb around the frequency f_{CW}. The whole absorption spectrum is obtained by scanning the frequency of the CW.

Frequency tuning and locking

The CW frequency is scanned and locked through the frequency scanning and locking module. The changing beat frequency represents the change in CW frequency. As shown in Fig. 3a, the beat frequency keeps stable in the locking process of frequency steps f_1, f_2, and f_3. The recorded frequency fluctuation is statistically analyzed and shown in Fig. 3b. The statistical standard deviation is 1.06 MHz in an integration time of 50 s for data acquisition. In the CW frequency scanning process, the beat frequency is changing periodically as shown in Fig.3c, d. Through the periodical trajectory, one can calculate the absolute frequency interval between the frequency steps. Since the beat signal between the CW laser and the optical frequency comb presents a triangular wave, the number of peaks and valleys in the triangular wave can be used to automatically determine how to calculate the scanning interval frequency. There are three kinds of frequency intervals. Case 1: the number of peaks is

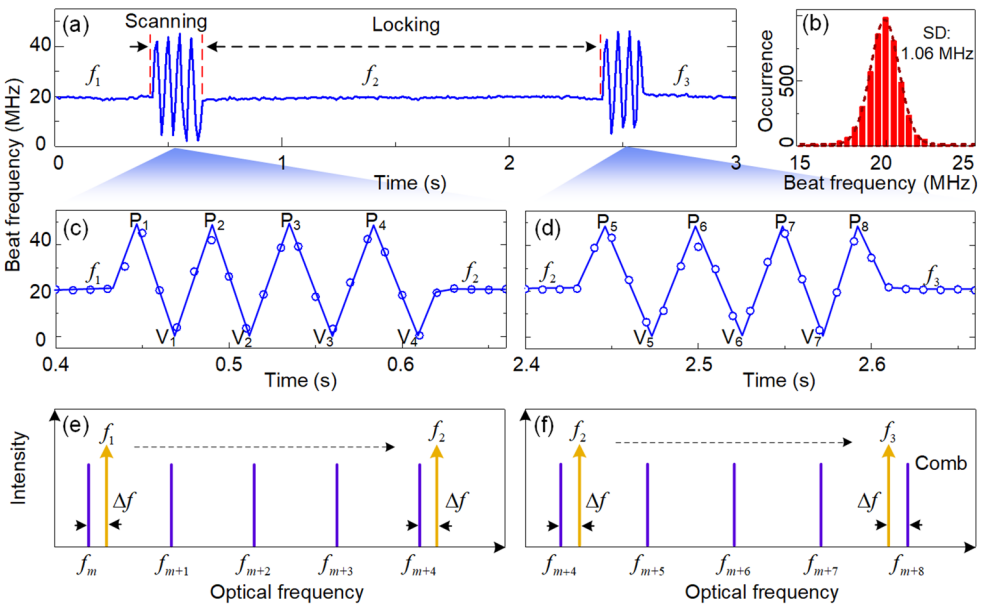

Fig. 3 CW laser scanning and locking processes. **a** The change in beat frequency. **b** Statistical histogram of the beat frequency in the locking process. *SD* Standard deviation. **c**, **e** The enlarged scanning process from f_1 to f_2. *P* peak, *V* valley. **d**, **f** The enlarged scanning process from f_2 to f_3

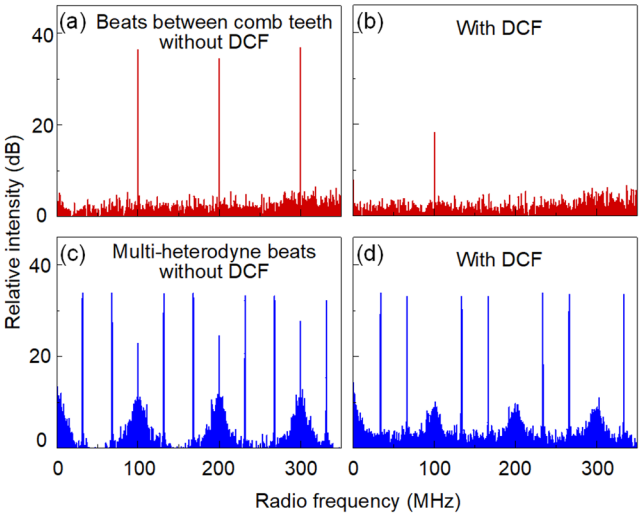

Fig. 4 **a**, **b** RF spectrum of the heterodyne detection between two comb teeth when the femtosecond pulses are stretched or not stretched by DCF. **c**, **d** RF spectrum of the comb-CW multi-heterodyne detection when the femtosecond pulses are stretched or not stretched by DCF

equal to the number of valleys. The frequency interval can be expressed as Mf_r, where M is the number of peaks. Case 2: the number of peaks is greater than the number of valleys. The frequency interval is $Mf_r - 2\Delta f$. Case 3: the number of peaks is less than the number of valleys. The frequency interval is $Mf_r + 2\Delta f$. Figures 3c, e show the changes in beat frequency and CW frequency of case (1) The CW frequency changing from f_1 to f_2, and it is always on the right side of the nearest comb tooth. Figure 3d, f show the changes in beat frequency and CW frequency of case (2) The location of the CW frequency is changed from the right side to the left side of nearest comb tooth. While in case 3, the location of the CW frequency is changed from the left side to the right side of nearest comb tooth. So that the frequency interval is $Mf_r + 2\Delta f$.

Suppression of the beats between comb teeth

In the multi-heterodyne detection, the RF spectral lines generated between comb teeth are usually larger in intensity than the beats between comb and CW but contain no spectrum information. They can be suppressed by balanced detection [15], but not eliminated in our experiment. After stretching the femtosecond laser pulses by DCF, the beats between the comb teeth can be further suppressed. Figure 4a, b show the RF spectrum of the heterodyne detection between comb teeth, in which the CW laser is not involved. The RF spectral lines at frequencies of 200 MHz and 300 MHz are suppressed.

down to the noise level after the comb transmits through the DCF (Fig. 4b). The residual line at 100 MHz represents the repetition rate of the interference signal. As well, the beats of the comb teeth in the multi-heterodyne detection between comb and CW are suppressed down to noise level with the stretched pulses as shown in Fig. 4b.

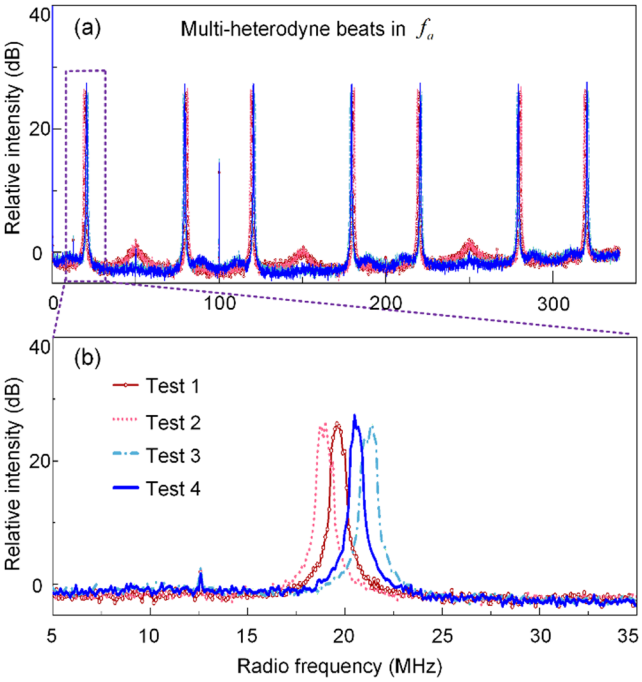

Fig. 5 **a** Four tests of the multi-heterodyne beats generated in frequency step f_a. **b** Zoom-in image of **a** from 5 to 35 MHz

Wideband searching and precise detecting modes

Figure 5 illustrates the multi-heterodyne beat notes in one locking step. Four tests in the enlarged as shown in Fig. 5b shows that the obtained RF comb teeth are distributed around the theoretical locking frequency. Every test is acquired by averaging 100 measurement times, and the single measurement takes 1 µs. The SNR of the averaged signal is 30 dB in f_a, which is located in the absorption peak. It is higher than 35 dB in the non-absorption location. Then, the peaks of the four tests in Fig. 5b are extracted and averaged. The other peaks in Fig. 5a are processed in the same way. Finally, The averaged 7 comb peaks are unfolded to recover the optical frequency comb spectrum information around the CW frequency f_a.

In practical optical spectrum detection, one usually should search for a wide spectrum to find the absorption spectrum first. And then a precise measurement is carried out on a determined absorption line. Thanks to the programmable frequency scanning and locking process, wideband searching and precise analyzing modes are switchable in our system. Figure 6a shows the wideband searching results of a $H^{13}CN$ gas cell with a length of 48 cm and pressure of

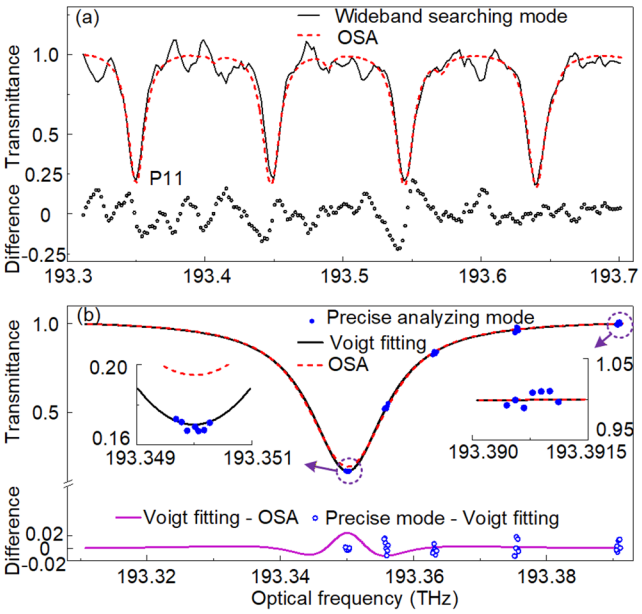

Fig. 6 Measurement results in wideband searching mode (**a**) and precise analyzing mode (**b**). Upper figure in **b**: Precise analyzing mode with five locked frequency steps. Bottom figure in **a**: the transmittance difference between the results from wideband searching mode and OSA. Bottom figure in **b**: the transmittance difference between the results from precise analyzing mode and Voigt fitting, the difference between the results from Voigt fitting and OSA

100 torr at a laser wavelength scanning speed of 0.1 nm/s. The obtained spectrum is smoothed with.

a window of 10 GHz. Its fluctuation is due to the unstable frequency of the free-scanning CW laser. Anyway, the searching results show good agreement with the measurement of an optical spectrum analyzer (OSA) with a resolution of 0.02 nm with red dashed line in Fig. 6a. The bottom dots of Fig. 6a are the difference of obtained spectrum between the precise detecting mode and OSA, which demonstrate the detection performance of this mode. The maximum deviation is 0.22, and the frequency resolution is 1.82 GHz at the scanning speed of 12.5 GHz/s. After that, the program is tuned to precise analyzing mode.

In precise analyzing mode, five frequency steps f_a, f_b, f_c, f_d, and f_e are chosen to sample the absorption line P11. The intervals between the adjacent frequency steps are 5.76 GHz, 7.34 GHz, 12.3 GHz, and 15.3 GHz, which are calculated from the trajectory of the beat frequency in the frequency scanning and locking module, as mentioned in Fig. 3. The multi-heterodyne beats in the frequency step f_a are shown in Fig. 5a. 7 comb peaks are unfolded from the raw multi-heterodyne beats in each frequency step, which means that 35 peaks (blue dots in Fig. 6b) are used to analyze this absorption line. Although one can employ more frequency steps to sample the absorption line densely, it will take more time for frequency scanning and locking. Thanks to the highly stable frequency during the locking process and the accurate frequency scanning intervals, the chosen five steps are enough to fit the absorption line under test. The spectrum resolution is equal to the comb tooth spacing of 100 MHz. The black line in Fig. 6b shows the Voigt fitting of the measured 35 peaks. The insets and the bottom of Fig. 6b demonstrate the detection accuracy of the precise detecting mode. The maximum deviation and maximum relative deviation are 0.018 and 3%, respectively. In addition, the measurement of OSA in the red dashed line gives further proof. While the OSA shows not enough spectrum resolution in the peak of the absorption line, as shown in the left inset of Fig. 6b.

Conclusion

In conclusion, we have developed a comb multi-heterodyne spectroscopy system with a low acquisition bandwidth for wideband absorption spectrum analysis. A universal spectrum analysis procedure was proposed, consisting of two operation modes: a wideband searching mode and a precise analyzing mode. In the wideband searching mode, the maximum deviation is 0.22, and the frequency resolution is 1.82 GHz at a scanning speed of 12.5 GHz/s. In the precise analyzing mode, the maximum deviation, frequency resolution and acquisition time in each scanning step are 0.018, 100 MHz and 400 µs, respectively. These programmed modes ensure that the proposed multi-heterodyne spectroscopy can be effectively applied to practical scenarios involving unknown spectrum analysis. In future work, the stretched femtosecond pulses can be further amplified to enable long-range atmospheric gas detection.

Supplementary Information The online version contains supplementary material available at https://doi.org/10.1007/s12596-025-02990-3.

Acknowledgements The authors thank the editor and reviewers for their valuable comments on the paper.

Funding National Natural Science Foundation of China (42305147); Natural Science Foundation of Jiangsu Province (BK20230428).

Conflict of interest The authors declare no Conflict of interest.

References

1. T. Fortier, E. Baumann, 20 years of developments in optical frequency comb technology and applications. Commun. Phys. **2**(1), 1–16 (2019)
2. N. Picqué, T.W. Hänsch, Frequency comb spectroscopy. Nat. Photonics. **13**(3), 146–157 (2019)
3. S.T. Cundiff, A.M. Weiner, Optical arbitrary waveform generation. Nat. Photonics **4**(11), 760–766 (2010)

4. I. Coddington, W.C. Swann, N.R. Newbury, Coherent multiheterodyne spectroscopy using stabilized optical frequency combs. Phys. Rev. Lett. **100**(1), 11–14 (2008)
5. I. Coddington, N. Newbury, W. Swann, Dual-comb spectroscopy. Optica. **3**(4), 414 (2016)
6. S.M. Link, D.J.H.C. Maas, D. Waldburger, U. Keller, Dual-comb spectroscopy of water vapor with a free-running semiconductor disk laser. Science. **356**(6343), 1164–1168 (2017)
7. T. Ideguchi, T. Nakamura, Y. Kobayashi, K. Goda, Kerr-lens mode-locked bidirectional dual-comb ring laser for broadband dual-comb spectroscopy. Optica. **3**(7), 748 (2016)
8. Z. Zhang, H. Xia, S. Yu, L. Zhao, T. Wei, M. Li, Femtosecond imbalanced time-stretch spectroscopy for ultrafast gas detection. Appl. Phys. Lett. **116**(17), 171106 (2020)
9. G. Millot, S. Pitois, M. Yan, T. Hovhannisyan, A. Bendahmane, T.W. Hänsch, N. Picqué, Frequency-agile dual-comb spectroscopy. Nat. Photonics. **10**(1), 27–30 (2016)
10. X. Yan, X. Zou, W. Pan, L. Yan, J. Azaña, Fully digital programmable optical frequency comb generation and application. Opt. Lett. **43**(2), 283 (2018)
11. M.-G. Suh, Q.-F. Yang, K.Y. Yang, X. Yi, K.J. Vahala, Microresonator soliton dual-comb spectroscopy. Science. **354**(6312), 600–603 (2016)
12. K. Urabe, O. Sakai, Absorption spectroscopy using interference between optical frequency comb and single-wavelength laser. Appl. Phys. Lett. **101**(5), 1–5 (2012)
13. Y. Wang, X. Ren, K. Huang, M. Yan, H. Zeng, Frequency comb interference spectroscopy using a fiber laser comb and a multicolour laser. Laser Phys. (2020). https://doi.org/10.1088/1555-6611/ab85c8
14. J. Lee, K. Lee, J. Yang, Y.-J. Kim, S.-W. Kim, Comb segmentation spectroscopy for rapid detection of molecular absorption lines. Opt. Express. **27**(6), 9088 (2019)
15. T. Hasegawa, H. Sasada, Direct-comb molecular spectroscopy by heterodyne detection with continuous-wave laser for high sensitivity. Opt. Express. **25**(16), A680 (2017)
16. K. Urabe, O. Sakai, Multiheterodyne interference spectroscopy using a probing optical frequency comb and a reference single-frequency laser. Phys. Rev. - Mol. Opt. Phys. **88**(2), 1–5 (2013)
17. L. Zhao, H. Xia, Y. Hu, T. Wu, Z. Zhang, J. Han, Y. Wu, T. Luo, Time-stretched femtosecond lidar using microwave photonic signal processing. J. Light Technol. **38**(22), 6265–6271 (2020)
18. H. Xia, C. Zhang, Ultrafast and doppler-free femtosecond optical ranging based on dispersive frequency-modulated interferometry. Opt. Express **18**(5), 4118 (2010)
19. G. Wang, Z. Yan, L. Yang, L. Zhang, C. Wang, Improved resolution optical time stretch imaging based on high efficiency in-fiber diffraction. Sci. Rep. **8**(1), 1–9 (2018)
20. X. Liu, X. Yao, Y. Cui, Real-time observation of the buildup of soliton molecules. Phys. Rev. Lett. **121**(2), 23905 (2018)
21. M. Li, Y. Song, C. Zhang et al., Generation and observation of multiple solitons from a mid-infrared ultrafast fiber laser. Chin. Opt. Lett. **22**(3), 031405 (2024)